

Approximation of the Time-Dependent Electronic Schrödinger Equation by MCTDHF^{*}

Othmar Koch, Wolfgang Kreuzer, Armin Scrinzi

Vienna University of Technology, Austria

Abstract

The numerical approximation of the solution of the time-dependent Schrödinger equation arising in ultrafast laser dynamics is discussed. The linear electronic Schrödinger equation is reduced to a computationally tractable, lower dimensional system of nonlinear partial differential equations by the *multi-configuration time-dependent Hartree-Fock method (MCTDHF)*. This method uses an ansatz for the wave function on a nonlinear manifold, taking into account the antisymmetry inherent in the model to reduce the dimension of the solution space. We show that the ansatz used is consistent with the original equation and the solution can be represented exactly in principle using the solutions of the nonlinear PDEs associated with MCTDHF. For the practical solution of the MCTDHF equations, several numerical techniques are discussed, and it is demonstrated that physically relevant problems can be solved satisfactorily.

Key words: Time-dependent Schrödinger equation, ultrafast laser dynamics, variational approximation, Dirac-Frenkel principle, multi-configuration time-dependent Hartree-Fock method, method of lines, pseudospectral method, Runge-Kutta methods, splitting methods

^{*} This project was supported by SFB F011 “AURORA” and SFB F016 “ADLIS” of the Austrian Science Fund FWF, and SFB 382 at the University of Tübingen, Germany.

Email addresses: othmar@othmar-koch.org (Othmar Koch),
kreuzer@aurora.anum.tuwien.ac.at (Wolfgang Kreuzer),
scrinzi@tuwien.ac.at (Armin Scrinzi).

1 Introduction

In this paper we discuss analytical and numerical properties of a new approach for the numerical solution of the time-dependent electronic Schrödinger equation (TDSE) arising in ultrafast laser dynamics, which was first proposed in [1], [2].

Large-scale computations of electronic structure and dynamics pose extremely challenging problems in several areas of research. For static electronic structure computations, many different methods have been developed in various fields, such as theoretical physics or theoretical and computational chemistry. As computationally cheaper alternatives to the solution of the time-independent Schrödinger equation by direct discretization, methods like *density functional theory (DFT)* or *(multi-configuration) Hartree-Fock (MCHF)* are being used.

DFT is a powerful method to reduce the Schrödinger equation for f degrees of freedom from a linear problem in \mathbb{R}^{3f} to a set of f nonlinear equations in \mathbb{R}^3 , where the computational effort is proportional to f^2 . DFT has found its most prominent applications in the calculation of ground-state properties of systems with many particles such as solids. MCHF, in turn, is one of the most powerful standard tools in electronic structure calculations of atoms and small molecules. Similar to DFT, MCHF reduces the Schrödinger equation to a coupled set of nonlinear equations, but with computational effort proportional to N^4 , for some $N \geq f$ occurring in the specification of the method. For few particle systems, this entails a tolerable increase of computational effort. In contrast to DFT, increasing N allows to, in principle, systematically improve the approximation of the original Schrödinger equation by MCHF. In both, DFT and MCHF, (nonlinear) *eigenvalue problems* have to be solved.

Ultrashort strong laser pulses, however, require the solution of time-dependent *initial value problems*. These laser pulses developed during the last few years have opened a new regime in the interaction of fields with matter [3], [4], [5]. One of the most intriguing aspects is the possibility of ultrashort time-resolved spectroscopy in the sub-femtosecond time domain.

For the solution of the time-dependent problems, different levels of approximation have been used, which range between the direct discretization of the TDSE as the most precise but computationally most expensive choice, and time-dependent density functional theory (TDDFT), which is appealing from a computational point of view but turned out to be too crude an approximation to capture important features of the problem, see below.

The present state of the art of numerically solving the time-dependent Schrödinger equation directly for realistic laser pulses is limited to two electron systems. The most successful calculations involve the largest massively parallel

computers available [6], [7]. It is clear that the direct solution of the linear time-dependent Schrödinger equation has reached its computational limits.

The use of TDDFT for this problem is limited at least by two drawbacks: The known approximations of the crucial “exchange correlation” term, while producing consistent ground state energies, generate contradictory and incorrect dynamical behavior [8] and there is no applicable theory for the description of multi-electron processes, such as detachment of two electrons from an atom. While this approach promises an enormous reduction in the complexity of the computational problems, the theory is not yet developed far enough so as to be applicable to our problem, see also [1].

Therefore the best choice at present to make the original, linear Schrödinger equation tractable for numerical computation is the multi-configuration time-dependent Hartree-Fock method (MCTDHF) proposed in [1], [2], [9]. This approach produces a lower-dimensional, nonlinear system of coupled Schrödinger equations. The method excels in its favorable computational complexity in relation to the number of particles in the model, thus making a simulation of systems with up to ten particles feasible, see [2]. In both the computational effort and the accuracy of the approximation MCTDHF is a compromise between the direct solution of the problem and TDDFT, and makes it possible to solve even highly correlated systems within acceptable computation time.

2 Model equations and the MCTDHF ansatz

We study the solution of the time-dependent Schrödinger equation for an atom or molecule with f degrees of freedom in a time-dependent electric field (typically arising from ultrashort laser pulses),

$$i\frac{\partial\psi}{\partial t} = H\psi, \quad (1)$$

where the complex-valued *wave function* $\psi = \psi(q_1, \dots, q_f, t)$ explicitly depends on time t and generalized coordinates $q_i = (s_i, x_i)$, where x_i is the spatial coordinate and $s_i = \pm 1/2$ denotes the spin of the i -th electron in an atom or molecule. The Hamiltonian H is time-dependent and has the form

$$H := \sum_{k=1}^f \left(\frac{1}{2} (-i\nabla_k - A(t))^2 + U(x_k) + \sum_{l \neq k} V(x_k - x_l) \right), \quad (2)$$

where

$$U(x) := -\sum_{l=1}^f U_1 \left(x - 1.4 \left(l - \frac{f+1}{2} \right) \right), \quad U_1(x) = \frac{1}{\sqrt{a^2 + x^2}}, \quad (3)$$

$$V(x-y) := \frac{1}{\sqrt{1 + (x-y)^2}}, \quad (4)$$

$$A(t) := e^{-(t/\tau)^2} \sin(\omega t) A_0. \quad (5)$$

∇_k is the nabla operator w.r.t. x_k only. For this potential, the internuclear distance is fixed at 1.4, and for each molecule the screening parameter a is adjusted such that the ionization potential is 0.3 independent of f [1], [2]. For instance, for $f = 2$, this means that $a = 1.28$, and for $f = 4$, $a = 1.283$ holds. Moreover, ω is of order of magnitude 10^{-1} , $\tau = \frac{2\pi}{\omega}\mu$, where $\mu \in \mathbb{R}$ is of order of magnitude 10, and A_0 is a constant, $A_0 = O(1)$. It is important to note that $H = H(x_1, \dots, x_f, t)$ is symmetric under the exchange of any two of its arguments x_i, x_j and does not depend on electron spin. For the moment, we restrict ourselves to problems in one space dimension to demonstrate the feasibility of our approach. The extension to cylindrically symmetric problems in three dimensions is work in progress.

The multi-electron wave function ψ from (1) is approximated by a function satisfying the ansatz

$$\begin{aligned} \psi(q_1, \dots, q_f, t) &= \sum_{(j_1, \dots, j_f)} a_{j_1, \dots, j_f}(t) \tilde{\phi}_{j_1}(q_1, t) \cdots \tilde{\phi}_{j_f}(q_f, t) \\ &= \sum_{(j_1, \dots, j_f)} a_{j_1, \dots, j_f}(t) \phi_{j_1}(x_1, t) \cdots \phi_{j_f}(x_f, t) |s_{j_1}\rangle \otimes \cdots \otimes |s_{j_f}\rangle \\ &=: \sum_J a_J(t) \Phi_J(x, t) S. \end{aligned} \quad (6)$$

The notation in (6) should be interpreted as follows: $|s_{j_i}\rangle$ denotes a column vector in two dimensions with the label $s_{j_i} = \pm 1/2$, where

$$|1/2\rangle = \begin{pmatrix} 1 \\ 0 \end{pmatrix} \quad (\text{“up”}), \quad |-1/2\rangle = \begin{pmatrix} 0 \\ 1 \end{pmatrix} \quad (\text{“down”}).$$

Thus, the repeated Kronecker products \otimes mean that the dimension of the system of equations to be solved is multiplied by 2^f , where each instance represents a possible combination of spins $\pm 1/2$ associated with the f electrons which can be propagated independently of the other equations. It is sufficient to consider *single-particle functions* $\phi_j = \phi_j(x_k, t)$ which only depend on position and time, as the Hamiltonian H does not depend on spin, either. Thus, our subsequent discussion can proceed without taking into account spin explicitly.

In (6), the *Pauli principle* [10] implies a restriction to solutions ψ which are antisymmetric under exchange of any two of their arguments q_j, q_k . This assumption is particular to the MCTDHF approach, as compared with the *multi-configuration time-dependent Hartree method (MCTDH)* considered, for example, in [11], [12] or [13], and reduces the number of equations considerably. Particularly, the assumption implies antisymmetry in the coefficients a_J . Formally, multiindices $J = (j_1, \dots, j_f)$ vary for $j_k = 1, \dots, N, k = 1, \dots, f$. Due to the simplifications resulting from antisymmetry, only $\binom{N}{f}$ equations for a_J have to be solved in the actual computations, however. The difference between the number of electrons with spin up and spin down is set as an initial condition and it remains constant throughout propagation, as our equations do not explicitly depend on spin. Typical initial conditions for energetically low lying states are such that this difference is minimal, i. e., 0 for an even number of electrons and 1 for an odd number. In spite of the actual reduction of the dimension of the systems we need to solve, we keep this description close to [11] for convenience of notation. We will demonstrate below that antisymmetry is preserved by the full MCTDH equations, and thus no unnecessary complications are introduced by this approach.

The Frenkel-Dirac variational principle [14], [15] is used to derive differential equations for the coefficients a_J and the *single-particle functions* ϕ_k . Thus, for ψ in the manifold

$$\mathcal{M} = \left\{ \psi : \psi(x, t) = \sum_J a_J(t) \phi_{j_1}(x_1, t) \cdots \phi_{j_f}(x_f, t) \right\},$$

where $a_J \in \mathbb{C}$ and $\phi_{j_k} \in L^2_1$ (the Hilbert space L^2 w. r. t. one spatial variable), we require

$$\left\langle \delta\psi \left| i \frac{\partial}{\partial t} - H \right| \psi \right\rangle_{L^2_f} = 0, \quad (7)$$

where $\delta\psi$ varies in the tangent space $\mathcal{T}_\psi \mathcal{M}$ of \mathcal{M} at ψ ,

$$\mathcal{T}_\psi \mathcal{M} = \left\{ \delta\psi : \delta\psi(x, t) = \sum_J \left(\delta a_J \Phi_J(x, t) + a_J \sum_{k=1}^f \delta\phi_{j_k}(x_k) \prod_{l \neq k} \phi_{j_l}(x_l) \right) \right\},$$

with $\delta a_J \in \mathbb{C}$ and $\delta\phi_{j_k} \in L^2_1$. By $\langle \cdot | \cdot \rangle_{L^2_f}$ we denote the usual scalar product in L^2 w. r. t. f spatial variables¹. Note that (7) implies that the residual

¹ Recall that for an operator H ,

$$\langle \psi | H | \tilde{\psi} \rangle_{L^2_f} = \langle \psi | H \tilde{\psi} \rangle_{L^2_f} = \int_{\mathbb{R}} \cdots \int_{\mathbb{R}} \bar{\psi}(H \tilde{\psi}) dx_1 \cdots dx_f.$$

$\|i\partial\psi/\partial t - H\psi\|$ is minimal in \mathcal{M} , see [16].

In order to define a unique solution of (7), we impose additional constraints,

$$\langle \phi_j | \phi_k \rangle_{L_1^2} = \delta_{j,k}, \quad t = 0, \quad (8)$$

$$\left\langle \phi_j \left| \frac{\partial \phi_k}{\partial t} \right. \right\rangle_{L_1^2} = -i \langle \phi_j | g | \phi_k \rangle_{L_1^2}, \quad t \geq 0, \quad (9)$$

where we have the freedom of choice to use any self-adjoint operator g . Usually, we set $g \equiv 0$ for reasons of simplicity. The requirement (8) together with (9) guarantees that

$$\langle \phi_j | \phi_k \rangle_{L_1^2} = \delta_{j,k}, \quad t > 0. \quad (10)$$

To see this, it is sufficient to show

$$\frac{d}{dt} \langle \phi_j | \phi_k \rangle_{L_1^2} = 0.$$

This relation can easily be proven using (9) and taking into account the fact that g is self-adjoint:

$$\begin{aligned} \frac{d}{dt} \langle \phi_j | \phi_k \rangle_{L_1^2} &= \left\langle \phi_j \left| \frac{\partial \phi_k}{\partial t} \right. \right\rangle_{L_1^2} + \left\langle \frac{\partial \phi_j}{\partial t} \left| \phi_k \right. \right\rangle_{L_1^2} \\ &= \left\langle \phi_j \left| \frac{\partial \phi_k}{\partial t} \right. \right\rangle_{L_1^2} + \overline{\left\langle \phi_k \left| \frac{\partial \phi_j}{\partial t} \right. \right\rangle_{L_1^2}} \\ &= -i \langle \phi_j | g | \phi_k \rangle_{L_1^2} + i \overline{\langle \phi_k | g | \phi_j \rangle_{L_1^2}} \\ &= -i \langle \phi_j | g | \phi_k \rangle_{L_1^2} + i \langle \phi_j | g | \phi_k \rangle_{L_1^2} \\ &= 0. \end{aligned}$$

The variational principle (7) and the additional restrictions (8) and (9), finally yield the “working equations”

$$i \frac{da}{dt} = A_H(\phi)a, \quad (11)$$

$$i \frac{\partial \phi}{\partial t} = B_H(a, \phi)\phi, \quad (12)$$

for $a = (a_{j_1, \dots, j_f})$, $\phi = (\phi_k)$. In equation (11),

$$[A_H(\phi)]_{J,L} := \langle \Phi_J | H | \Phi_L \rangle_{L_f^2} \quad (13)$$

is a ‘‘Galerkin matrix’’, and (12) is derived from

$$i\rho \frac{\partial \phi}{\partial t} = (I - P)\overline{H}\phi, \quad (14)$$

where

$$\psi_j := \langle \phi_j | \psi \rangle_{L_1^2}, \quad (\text{‘‘single-hole functions’’}), \quad (15)$$

$$\rho_{j,l} := \langle \psi_j | \psi_l \rangle_{L_{f-1}^2}, \quad (\text{‘‘density matrix’’}), \quad (16)$$

$$\overline{H}_{j,l} := \langle \psi_j | H | \psi_l \rangle_{L_{f-1}^2}, \quad (\text{‘‘mean field operator matrix’’}), \quad (17)$$

and P is the orthogonal projector onto the space spanned by the functions ϕ_k . Note that the mean-field operator matrix from (17) contains operators acting on one spatial variable, respectively.

The equivalence of (12) and (14) is not trivial and requires some further discussion. In cases where the density matrix ρ is singular a special treatment is necessary, see [11], [17]. We do not consider this case here, as it rarely occurs in practice when the initial state is chosen sensibly.

It must be stressed at this point that it is not necessary to enforce antisymmetry of the solution during the time integration of (11), (12). If the initial state at $t = 0$ is chosen as

$$\psi_0(x_1, \dots, x_f) = \sum_J a_J \phi_{j_1}(x_1) \cdots \phi_{j_f}(x_f) \quad (18)$$

such that ψ_0 is antisymmetric, and a_J , $\phi_{j_k}(x_k)$ serve as initial values for (11) and (12), respectively, antisymmetry is preserved since H is symmetric under the exchange of any two of its arguments.

To see that the solution of the full TDSE (1) has the property to preserve antisymmetry of the initial state, it is sufficient to show that the function

$$y_{i,j}(x, t) := \psi(x, t) + P_{i,j}\psi(x, t),$$

where the operator $P_{i,j}$ swaps the arguments x_i and x_j of a function, is an invariant of motion for a solution of (1) and any i, j . Note that $P_{i,j}$ is self-adjoint. This follows from the Theorem of Fubini [18] on realizing that we only

have to change the integration order in the inner product $\langle \cdot | \cdot \rangle_{L_f^2}$. Now, we use the fact that $P_{i,j}$ commutes with H , which implies

$$\begin{aligned} i \frac{\partial y_{i,j}}{\partial t} &= (I + P_{i,j})H\psi = H(I + P_{i,j})\psi = Hy_{i,j}, \\ y_{i,j}(x, 0) &= 0. \end{aligned}$$

If the original equation (1) defines a unique solution, we may now conclude that $y_{i,j} = 0$ for all t and any i, j . In the case where $A(t) = 0$, this follows from Stone's Theorem, as the differential operator is self-adjoint in that case and $U + V \in L_f^2$ is real [19].

The result for the solutions of the working equations (11) and (12) can be proven similarly: If we denote by $p_{i,k}(J)$ the operator swapping the indices j_i and j_k in the multiindex $J = (j_1, \dots, j_f)$, then $z_{i,k}^J(t) := a_J(t) + a_{p_{i,k}(J)}(t)$ satisfies

$$\begin{aligned} iz_{i,k}^J &= \sum_K \langle \Phi_J + \Phi_{p_{i,k}(J)} | H | \Phi_K \rangle_{L_f^2} a_K = \sum_K \langle (I + P_{i,k})\Phi_J | H | \Phi_K \rangle_{L_f^2} a_K \\ &= \sum_K \langle \Phi_J | H | (I + P_{i,k})\Phi_K \rangle_{L_f^2} a_K = \sum_K \langle \Phi_J | H | \Phi_K \rangle_{L_f^2} (a_K + a_{p_{i,k}(K)}) \\ &= \sum_K \langle \Phi_J | H | \Phi_K \rangle_{L_f^2} z_{i,k}^K, \\ z_{i,k}^J(0) &= 0, \end{aligned}$$

since $P_{i,k}$ is self-adjoint and commutes with H . Thus, $z_{i,k}^J(t) = 0$, $t > 0$, and antisymmetry in the initial Hartree product (18) is reflected in the coefficients a_J for all t . As an important consequence, it is possible to use the calculus developed for setting up the equations in MCTDH, and apply the simplifications resulting from antisymmetry to reduce the dimension of the system likewise for all t . Thus, the working equations constructed in this way remain valid and produce the antisymmetric solution for all t .

Consequently, theoretical results on the existence and uniqueness of the solution of the working equations also carry over from the case of MCTDH to the Hartree-Fock equations (11) and (12). It was shown in [20] that when $A(t) = 0$ in (2) and the potential is smooth, there is a unique solution of the working equations in the Sobolev space H^2 .

As an extension of the model which is important in practical computations we introduce a *complex absorbing potential (CAP)*. The CAP is used to eliminate an undesirable solution behavior not related to the physical situation, which may be introduced by periodic boundary conditions on a truncated spatial interval $[-x_{\text{end}}, x_{\text{end}}]$. In [11], a complex absorbing potential similar to the one

we use is suggested to cope with these problems. In one space dimension, our CAP is defined as an artificial contribution to the Hamiltonian H of the form

$$w(x) := -i\frac{c}{2} \left(1 - \cos \left(\pi \frac{|x - c_{\text{end}}|}{x_{\text{end}} - c_{\text{end}}} \right) \right), \quad |x| > c_{\text{end}}, \quad (19)$$

which vanishes for $|x| \leq c_{\text{end}}$.

As it is cumbersome, or even infeasible, to consider the values of the wave function ψ , or alternatively the coefficient vector a and single-particle functions ϕ , for numerical comparisons for a larger number f of particles, we will instead use the *electron density*

$$\langle \psi | \psi \rangle_{L^2_{f-1}} = \int_{\mathbb{R}} \cdots \int_{\mathbb{R}} \bar{\psi} \psi dx_2 \cdots dx_f \quad (20)$$

to display our numerical results.

Before we turn to the discussion of numerical methods for the working equations (11) and (12), we show that using the ansatz (6) we could in principle represent the wave function ψ exactly by using an infinite number of configurations, and that the working equations are thus consistent with the TDSE in this respect.

Consider the solutions of the working equations (11) and (12). First, we note that (12) implies that (9) holds with $g \equiv 0$ ². Thus, if the initial state is chosen according to (18) such that (8) is satisfied, then (10) follows for $N \in \mathbb{N}$. Now we consider the situation for $N = \infty$. If the initial state (18) is chosen as a complete orthonormal system³ consisting of functions in the Sobolev space H^2 , the same holds for any $t > 0$: It follows that $P = I$ in (12) and also $\partial\phi_j/\partial t = 0$ from (9). Consequently, ϕ_j are constant as a function of t and (12) is satisfied. Clearly now, for ψ there exists an expansion

$$\psi = \sum_J a_J \phi_{j_1} \cdots \phi_{j_f},$$

with the Fourier coefficients a_J w. r. t. (Φ_J) . We will subsequently demonstrate that ψ is the solution of (1) if and only if the coefficients a_J satisfy (11).

² We should point out at this point that using $g \neq 0$ in (9) results in a modification of the working equations [11].

³ For example,

$$\frac{1}{\sqrt{\pi}} \frac{1}{x + i} \left(\frac{x - i}{x + i} \right)^n$$

for $n \in \mathbb{Z}$ constitutes a complete orthonormal system in L^2_1 which can be used to construct (Φ_J) .

First, we have to show that the equation (11) is well-defined. For simplicity, we restrict ourselves to the case where $A(t) = 0$ in (2). Thus, H is a self-adjoint operator which maps H^2 into L_f^2 . Now, denote as h^2 the subset of ℓ^2 which consists of the Fourier coefficients w. r. t. (Φ_J) of functions from H^2 . The discrete operator A_H maps h^2 into ℓ^2 , and it is easy to see that A_H is selfadjoint in ℓ^2 because H is self-adjoint and L^2 and ℓ^2 are isomorphic. Moreover, we can use

$$H \sum_J a_J \Phi_J = \sum_J a_J H \Phi_J \quad (21)$$

because H is closed. Consequently, (11) has a unique solution in ℓ^2 .

Now, if we assume that $t \mapsto \psi(x, t)$ is differentiable w. r. t. t , that is,

$$\lim_{h \rightarrow 0} \left\| \frac{\psi(\cdot, t+h) - \psi(\cdot, t)}{h} - \dot{\psi}(\cdot, t) \right\|_{L_f^2} = 0,$$

then $a_J(t)$ are differentiable and represent the Fourier coefficients of $\dot{\psi}$. Consequently, we can write

$$i \frac{\partial \psi}{\partial t} = i \sum_J \dot{a}_J \Phi_J. \quad (22)$$

Thus, from (22) and (10), we conclude

$$\left\langle \Phi_J \left| i \frac{\partial \psi}{\partial t} \right\rangle_{L_f^2} = i \frac{da_J}{dt}, \quad (23)$$

and clearly from (21)

$$\langle \Phi_J | H \psi \rangle_{L_f^2} = \sum_K \langle \Phi_J | H | \Phi_K \rangle_{L_f^2} a_K. \quad (24)$$

Thus, (1) implies (11). Conversely, equations (23) and (24) can be used to conclude

$$\left\langle \Phi_J \left| i \frac{\partial \psi}{\partial t} - H \psi \right\rangle_{L_f^2} = 0, \quad \forall J$$

from (11), and (1) follows.

The last theoretical result shows that the working equations are consistent with the TDSE. The solution of (1) can in principle be represented exactly by functions satisfying (11) and (12). The practical question of the convergence

of the approximation given by MCTDHF is addressed empirically in [9]. In particular, the number of configurations necessary to achieve satisfactory accuracy for correlated, realistic models is demonstrated by practically relevant examples.

3 Numerical solution methods

To compute the solution of (11) and (12) numerically, the method of lines is used. First, space discretization is applied to derive a system of ordinary differential equations. To this end, we use the *pseudospectral method* [21], [22]. We found that this method is advantageous as compared with space discretization by low order finite differences. Firstly, the error decreases exponentially for smooth problems when the spatial grid is refined [21]. Moreover, the spectrum of the differential operator is approximated well even by the eigenvalues of its discretization with large modulus [23]. For numerical comparisons, see [24], [25].

As a prerequisite to introduce the pseudospectral method, we require some definitions. The *inverse discrete Fourier transform* of a discrete grid vector (which is assumed to depend on continuous time t) $\hat{U}(t) = (\hat{u}_{-K}(t), \dots, \hat{u}_{K-1}(t))$ is defined as

$$Z(x_l, t) := \text{DFT}^{-1}(\hat{U}) := \sum_{k=-K}^{K-1} \exp\left(\frac{ik\pi x_l}{x_{\text{end}}}\right) \hat{u}_k(t). \quad (25)$$

Here, we use an equidistant spatial grid (x_{-K}, \dots, x_K) defined on the truncated interval $[-x_{\text{end}}, x_{\text{end}}]$. Conversely, the *discrete Fourier transform* of $Z(x, t)$ is defined as

$$\hat{u}_k(t) := \text{DFT}(Z) := \frac{1}{2K} \sum_{l=-K}^{K-1} \exp\left(-\frac{ik\pi x_l}{x_{\text{end}}}\right) Z(x_l, t). \quad (26)$$

Now, the application of the kinetic part of the Hamiltonian H (which contains the derivatives w. r. t. the spatial variable) to a single-particle function $\phi_j(x, t)$ is approximated by

$$(-i\nabla - A(t))^2 \approx \text{DFT}^{-1} \circ (-iD - A(t))^2 \circ \text{DFT}, \quad (27)$$

where

$$D := \text{diag} \left(\frac{k\pi}{x_{\text{end}}} \right), \quad k = -K, \dots, K - 1.$$

By default, we use explicit Runge-Kutta methods for the time integration of the ODEs resulting after space discretization (27). For reasonably smooth data and moderate grid spacing Δx , these methods were found to work dependably and retain their classical convergence orders, thereby yielding an efficient method for time integration. Extensive test results reported in [24] support this claim, see also [25] and the examples given later in this section.

For difficult problems and fine spatial grids, however, a more robust, low-order alternative is given by *variational splitting* introduced in [13] for the nonlinear PDEs arising from MCTDH in quantum molecular dynamics.

In this method, the Hamiltonian $H := T + V$ from (2) is split into the parts

$$T := \sum_{k=1}^f \left(\frac{1}{2} (-i\nabla_k - A(t))^2 + U(x_k) \right), \quad (28)$$

$$V := \sum_{k=1}^f \sum_{l \neq k} V(x_k - x_l). \quad (29)$$

One step of the variational splitting method starting at $t = t_0$ with time step Δt is defined as follows:

- (1) Compute $\psi_{1/2}^- \in \mathcal{M}$ as the solution at time $t_0 + \frac{1}{2}\Delta t$ of

$$\left\langle \delta\psi \left| i\frac{\partial}{\partial t} - T \right| \psi \right\rangle_{L_f^2} = 0 \quad \forall \delta\psi \in \mathcal{T}_\psi \mathcal{M}, \quad (30)$$

with initial value $\psi(t_0) = \psi_0$ (“ T step”).

- (2) Compute $\psi_{1/2}^+ \in \mathcal{M}$ as the solution at time $t_0 + \Delta t$ of

$$\left\langle \delta\psi \left| i\frac{\partial}{\partial t} - V \right| \psi \right\rangle_{L_f^2} = 0 \quad \forall \delta\psi \in \mathcal{T}_\psi \mathcal{M}, \quad (31)$$

with initial value $\psi(t_0) = \psi_{1/2}^-$ (“ V step”).

- (3) Compute $\psi_1 \in \mathcal{M}$ as the solution at time $t_0 + \Delta t$ of (30) with initial value $\psi(t_0 + 1/2\Delta t) = \psi_{1/2}^+$.

This symmetric splitting yields a second order approximation for the solution to the full problem (7) resulting from MCTDH with smooth data, see [13]. Our numerical test results indicate that this is also the case for MCTDHF for the electronic Schrödinger equation discussed here.

Now, since $T\psi \in \mathcal{T}_\psi \mathcal{M}$ for $\psi \in \mathcal{M} \cap H^2$, the two steps of the form (30) are equivalent to solving the Schrödinger equation

$$i \frac{\partial \psi}{\partial t} = T\psi \quad (32)$$

on the respective domains. If the initial function is chosen according to (18), (32) decouples into a set of single particle Schrödinger equations:

$$\frac{da_J}{dt} = 0, \quad \forall J, \quad (33)$$

$$i \frac{\partial \phi_j}{\partial t} = \frac{1}{2} (-i\nabla - A(t))^2 \phi_j + U \phi_j, \quad \forall j. \quad (34)$$

The second splitting step (31) leads to equations

$$i \frac{da}{dt} = A_V(\phi)a, \quad (35)$$

$$i \frac{\partial \phi}{\partial t} = B_V(a, \phi)\phi, \quad (36)$$

where A_V and B_V are defined analogously as in (11) and (12), using the operator V instead of H .

The single particle Schrödinger equations (33) and (34) are efficiently solved by the pseudospectral method in conjunction with the exponential midpoint rule [17], [22].

For the solution of the *reduced working equations* (35) and (36), various (second-order) schemes can be employed. It turned out that the choice of the numerical integrator for these equations is not critical, since the reduced working equations do not suffer from the unsmoothness introduced by the space discretization of the (unbounded) differential operator T . Two (implicit) schemes proposed in [13] and an explicit variation of these schemes were implemented and found to perform similarly [24].

It must be stressed at this point that the problems (33), (34) and (35), (36) can be solved independently, using coarser step sizes for the numerical approximation of the smooth subproblem (35), (36). This may imply a massive reduction in the computational effort in many situations [24], [25]. In the setting discussed here, however, this feature of variational splitting could not be exploited, the best results were obtained when step sizes were chosen the same for both subproblems.

To conclude this section, we give some numerical results demonstrating that both, Runge-Kutta methods and variational splitting, retain their classical

convergence orders when employed for time integration of the working equations, and assess the efficiency of the methods in a typical test situation. To this end, in Tables 1 and 2, we give the results for a model problem where $N = 4$, $f = 2$, and the pseudospectral method is used for space discretization on a uniform grid with $K = 500$. The complete problem specification is given in [24]. All the numerical computations reported in this paper were performed with the MCTDHF code [9] on a Compaq SC45, where the code was compiled with the Compaq Fortran 90 Compiler V5.5-1877-48BBF in IEEE double precision arithmetic with relative machine precision $\approx 1.11 \cdot 10^{-16}$. Table 1 gives, for the classical Runge-Kutta method of order four used with different values of the discretization parameter Δt , the absolute and relative errors in the electron density and empirical convergence orders p_{abs} and p_{rel} computed w. r. t. a highly accurate reference solution (where $\Delta t = 3.125 \cdot 10^{-4}$ was chosen), and additionally the number fcount of evaluations of the mean field operator matrix \overline{H} . This last value is a good indicator of the performance of the method, as this is the computationally most expensive part of the calculation⁴, and the runtime for problems with large N and f is directly proportional to the number fcount [24]. The absolute error is computed as the maximum of the error over the whole spatial grid for every t , where subsequently the maximum over all t is taken, while for the relative error the maximum over the spatial grid is taken at the end point of the time interval, see [24]. The same quantities are given for variational splitting in Table 2, where the same reference solution as before is used. The discretization parameter Δt is chosen such that the same values of fcount appear for both the Runge-Kutta method and variational splitting. We observe that the classical convergence orders four and two are retained, respectively, but the results for variational splitting appear more reliable. However, for like values of fcount, the accuracy of the solutions computed by the Runge-Kutta method clearly exceeds the accuracy achieved by variational splitting. Thus, for this test configuration, the Runge-Kutta method should be favored. However, we observed that for fine spatial grids, variational splitting may be able to compute a solution reliably where Runge-Kutta methods become unstable. In addition, when low accuracies are sufficient, variational splitting may be employed, since the step sizes for the Runge-Kutta method have to be chosen rather small in order to guarantee a reliable integration by this method. Finally, the efficiency of the solution by variational splitting might be increased by using a composition method [26] in order to raise the convergence order of the numerical approximation. The complete results of our numerical experiments are given in [24].

⁴ Note that in order to make the evaluation computationally tractable, the particle-particle potential is expanded into a suitably truncated sum of products of single-particle potentials, thus reducing the complexity of the integrals appearing in the definition of \overline{H} . For details of this procedure, see [9].

| Δt | abs. err | p_{abs} | rel. err | p_{rel} | fcount |
|------------|------------|------------------|------------|------------------|---------|
| 5.00E-03 | 2.3710E-09 | | 1.1149E-05 | | 176,000 |
| 2.50E-03 | 2.9849E-10 | 2.99 | 1.1826E-06 | 3.24 | 352,000 |
| 1.25E-03 | 1.9560E-11 | 3.93 | 7.2798E-08 | 4.02 | 704,000 |

Table 1
Numerical results for the Runge-Kutta method.

| Δt | abs. err | p_{abs} | rel. err | p_{rel} | fcount |
|------------|------------|------------------|------------|------------------|---------|
| 2.50E-03 | 1.9101E-07 | | 1.6862E-04 | | 176,000 |
| 1.25E-03 | 4.7738E-08 | 2.00 | 4.2136E-05 | 2.00 | 352,000 |
| 6.25E-04 | 1.1933E-08 | 2.00 | 1.0534E-05 | 2.00 | 704,000 |

Table 2
Numerical results for variational splitting.

4 A realistic example

To demonstrate the potential of our code, we now give results computed for realistic data. Thus, we show the electron density for a molecule with four electrons ($f = 4$), where $N = 6$ is used in the ansatz (6) and a complex absorbing potential with $c_{\text{end}} = 60$ and $c = 1$ is imposed. A spatial grid with $K = 500$ is used on the interval $[-100, 100]$. The time integration is performed for $t \in [0, t_{\text{end}}]$, where t_{end} denotes 15 *optical cycles* $2\pi/\omega$, see (5). The laser pulse is chosen such that its amplitude increases linearly for the first two cycles, remains constant for two cycles, and finally decays again linearly for two cycles. In the last nine cycles of the computation, no laser field is present. Figure 1 shows the profile of the electron density in normal scaling and additionally on a logarithmic scale, where the spatial interval is truncated to $[-20, 20]$. To show the effects more clearly, we give cross-sections of the plot from Figure 1 at $t = 0$, and after three, six and 15 optical cycles in Figure 2. The plots show the two main effects of the laser-molecule interaction. On the linear scale, one sees a significant modulation of the dominant central feature of the electron density in the oscillatory field: the density oscillates according to the forces exerted by the field, the molecule is polarized. The fact that polarization is rather pronounced is characteristic for molecules. After the field has passed, the central peak is reduced, which corresponds to ionization, i. e., the lasting removal of electrons from the molecule. The dynamics of this effect is only visible in the logarithmic scale representation of the density (Figure 1, right, and Figure 2). In the absence of the laser field, the electron density decays exponentially with the distance from the central peak. When ionization starts, electrons are removed to larger distances. Note, however, that this density remains comparatively low at a level of $\sim 10^{-4}$ of the central density even during the maximal field strength. In general, the effect that is

measured in the laboratory is a rather small effect on top of stronger, but only transient modulations. This explains the rather high numerical accuracy needed in this type of calculation. It has been shown [9] that ionization is in fact strongly dependent on the number of orbitals N used in the calculation. In the language of physics, this means that ionization of molecules is a process that involves significant electron correlation.

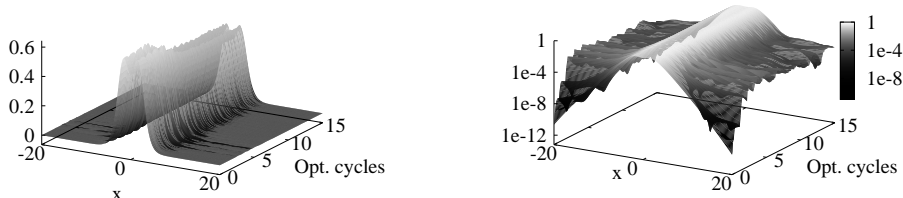


Fig. 1. Electron density for a realistic model showing polarization and ionization in normal scaling (left) and on a logarithmic scale (right).

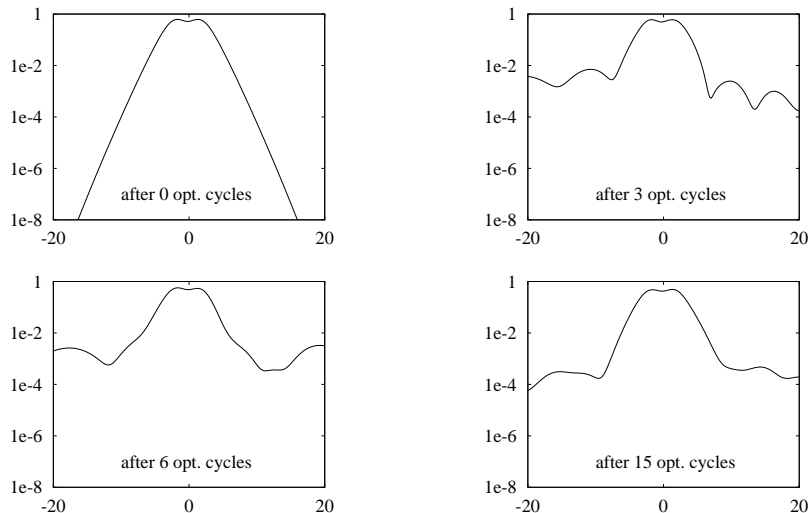


Fig. 2. Electron density for a realistic model showing polarization and ionization at $t = 0$, and after three, six and 15 optical cycles, logarithmic scale.

5 Conclusions and outlook

We have presented approximation methods for the solution of the time-dependent Schrödinger equation arising in ultrafast laser dynamics. We can show that the multi-configuration time-dependent Hartree-Fock method may serve to represent the wave function exactly in principle. Moreover, we proposed reliable numerical solution methods to be used in the context of the method of lines for the practical solution of the nonlinear PDEs associated

with MCTDHF, and assessed their applicability and performance. Our default choice for the numerical solution of the differential equations is space discretization by the pseudospectral method in conjunction with time integration by explicit Runge-Kutta methods, but variational splitting may yield a reliable alternative for time integration of unsmooth problems. Thus, a variable order, variable step size code based on these components is used to solve real-world problems, see also [1], [2], [9].

Our experiences so far suggest that our approach can also be successfully extended to problems in three spatial dimensions with cylindrical symmetry, which constitutes the physically relevant case. For an efficient implementation in that case, parallelization will be crucial in order to be able to solve large models. Consequently, the issue of space discretization will have to be reconsidered, and the time-stepping strategy may need to be refined. An extension of our code taking these aspects into account is currently being developed.

Acknowledgements

We wish to thank W. Auzinger, M. Kaltenbäck and C. Lubich for valuable hints on the topics of this paper.

References

- [1] J. Zanghellini, M. Kitzler, C. Fabian, T. Brabec, A. Scrinzi, An MCTDHF approach to multi-electron dynamics in laser fields, *Laser Physics* 13 (8) (2003) 1064–1068.
- [2] J. Zanghellini, M. Kitzler, T. Brabec, A. Scrinzi, Testing the multi-configuration time-dependent Hartree-Fock method, *J. Phys. B: At. Mol. Phys.* 37 (2004) 763–773.
- [3] F. Krausz, T. Brabec, Intense few-cycle laser fields: frontiers of nonlinear optics, *Rev. Mod. Phys.* 72 (2000) 545–562.
- [4] R. Kienberger, M. Hentschel, M. Uiberacker, C. Spielmann, M. Kitzler, A. Scrinzi, M. Wieland, T. Westerwalbesloh, U. Kleineberg, U. Heinzmann, M. Drescher, F. Krausz, Steering attosecond electron wave packets with light, *Science* 297 (2002) 1144–1148.
- [5] M. Drescher, M. Hentschel, R. Kienberger, M. Uiberacker, V. Yakovlev, A. Scrinzi, T. Westerwalbesloh, U. Kleineberg, U. Heinzmann, F. Krausz, Time-resolved atomic inner-shell spectroscopy, *Nature* 419 (2002) 803–807.

- [6] A. Bandrauk, A. Chelkowski, On laser Coulomb explosion imaging of proton motion, *Chem. Phys. Letters* 336 (2001) 518–522.
- [7] J. S. Parker, L. Moore, K. Taylor, Accurate computational methods for two-electron atom-laser interactions, *Optics-Express* 8 (2001) 436–441.
- [8] V. Veniard, R. Taieb, A. Maquet, Photoionization of atoms using time-dependent density functional theory, *Laser Physics* 13 (2003) 465–474.
- [9] J. Caillat, J. Zanghellini, M. Kitzler, W. Kreuzer, O. Koch, A. Scrinzi, Correlated multielectron systems in strong laser pulses - an MCTDHF approach, to appear in *Phys. Rev A* (2004).
- [10] L. D. Landau, E. M. Lifshitz, *Quantum Mechanics: Non-Relativistic Theory*, 3rd Edition, Pergamon Press, Oxford-New York, 1977.
- [11] M. H. Beck, A. Jäckle, G. A. Worth, H.-D. Meyer, The multiconfiguration time-dependent Hartree (MCTDH) method: A highly efficient algorithm for propagating wavepackets, *Phys. Rep.* 324 (2000) 1–105.
- [12] M. H. Beck, H.-D. Meyer, An efficient and robust integration scheme for the equations of the multiconfiguration time-dependent Hartree (MCTDH) method, *Z. Phys. D* 42 (1997) 113–129.
- [13] C. Lubich, A variational splitting integrator for quantum molecular dynamics, *Appl. Num. Math.* 48 (2004) 355–368.
- [14] P. Dirac, Note on exchange phenomena in the Thomas atom, *Proc. Cambridge Phil. Soc.* 26 (1939) 376–385.
- [15] J. Frenkel, *Wave Mechanics, Advanced General Theory*, Clarendon Press, Oxford, 1934.
- [16] C. Lubich, On variational approximations in quantum molecular dynamics, to appear in *Math. Comp.* (2003).
- [17] O. Koch, W. Kreuzer, A. Scrinzi, MCTDHF in ultrafast laser dynamics, AURORA TR-2003-29, Inst. for Appl. Math. and Numer. Anal., Vienna Univ. of Technology, Austria, available at <http://www.vcpc.univie.ac.at/aurora/publications/> (2003).
- [18] H. W. Alt, *Lineare Funktionalanalysis*, 3rd Edition, Springer Verlag, Berlin-Heidelberg-New York, 1999.
- [19] A. Pazy, *Semigroups of Linear Operators and Applications to Partial Differential Equations*, Springer-Verlag, New York, 1983.
- [20] T. Klett, *Regularität und Approximation im Multikonfigurations-Hartree-Verfahren der Quantendynamik*, Master Thesis, Eberhard Karls Universität Tübingen (2004).
- [21] L. Trefethen, *Spectral Methods in MATLAB*, SIAM, Philadelphia, 2000.

- [22] T. Jahnke, C. Lubich, Error bounds for exponential operator splittings, BIT 40 (2000) 735–744.
- [23] R. Kosloff, Quantum molecular dynamics on grids, in: R. E. Wyatt, J. Z. Zhang (Eds.), Dynamics of Molecules and Chemical Reactions, Marcel Dekker, New York, 1996, pp. 185–230.
- [24] O. Koch, W. Kreuzer, Performance of MCTDHF implementations, AURORA TR-2004-14, Inst. for Anal. and Sci. Comput., Vienna Univ. of Technology, Austria, available at <http://www.vcpc.univie.ac.at/aurora/publications/> (2004).
- [25] O. Koch, Numerical solution of the time-dependent Schrödinger equation in ultrafast laser dynamics, WSEAS Transactions on Mathematics 3 (2004) 584–590.
- [26] E. Hairer, C. Lubich, G. Wanner, Geometric Numerical Integration, Springer-Verlag, Berlin-Heidelberg-New York, 2002.